České vysoké učení technické v Praze, Fakulta stavební

Czech Technical University in Prague, Faculty of Civil Engineering

Ing. Petr Štemberk, Ph.D.

Modelování tuhnoucího betonu

Modeling of Concrete at Very Early Ages

Summary

The following work describes material modeling and experimental investigation of concrete at extremely early ages. At this age of hours, concrete microstructure is undergoing a rapid evolution which prohibits any assumption of constant material parameters in the modeling. As hydration is governing the strength development and other qualities of concrete considered in the design, the degree of hydration is chosen for description of concrete microstructure development. A concept similar to that proposed in the solidification theory is then used for definition of a material model for solidifying and further hardening concrete. An approach to extension of the range of applicability of the Chen model of plasticity also for the extremely early ages by defining the model parameters as functions of the degree of hydration is presented. Since consistency of concrete at such early ages is still rather soft, it prohibits application of testing equipment commonly used for the already hardened concrete. Suitable methods based on uniaxial testing are proposed along with a new technique for measurement of lateral deformation of concrete specimens using digital image processing. Application of the modified Chen model of plasticity and results obtained from experiments to solution of construction problems is demonstrated in two examples.

Souhrn

Předložená práce popisuje materiálové modelování a experimentální vyšetřování betonu velmi raného stáří. Ve stáří několika hodin prochází struktura betonu rychlým vývojem, kvůli kterému nelze považovat materiálové parametry užité v modelu za konstanty. Vzhledem k tomu, že hydratace řídí nárůst pevnosti a další vlastnosti betonu uvažované v návrhu železobetonových konstrukcí, byl stupeň hydratace zvolen pro popis vývoje struktury betonu v modelu. Solidifikační teorie je základem popisovaného materiálového modelu pro tuhnoucí a dále tvrdnoucí beton. Způsob rozšíření aplikovatelnosti modelu vytvořeného pro zatrvrdlý beton i pro beton tuhnoucí a dále tvrdnoucí je předveden na Chenově modelu plasticity, kdy uvažované materiálové parametry jsou definovány jako funkce stupně hydratace. Poněvadž konzistence betonu velmi raného stáří je velmi měkká, nelze použít zkušební zařízení běžně používané pro zkoušení ztvrdlého betonu. Proto jsou uvedeny vhodné metody pro zkoušení tuhnoucího a dále tvrdnoucího betonu vycházející z jednoosého zkoušení. Dále je navržena metoda pro měření příčné deformace zkušebních vzorků pomocí analýzy digitálních fotografií. Použití modifikovaného Chenova modelu plasticity a výsledků zkoušek pro řešení problémů při výstavbě je předvedeno na dvou příkladech.

Klíčová slova: tuhnoucí beton, tvrdnoucí beton, materiálový model, experimentální zkoušení

Keywords: solidifying concrete, hardening concrete, material model, experimental investigation

Table of contents

1. INTRODUCTION

The building industry is often used as an indicator of economy performance and as such it also suffers from today's global competition which is defined by the earliest least expensive delivery. This puts the building industry under enormous pressure to erect structures of standard quality swiftly and at low cost. In the case of concrete structures it means to use rapid hardening types of cement allowing earlier loading, however, which brings about all kinds of risk related to high temperature evolution usually manifested by cracks. Applying load at the extremely early ages may also lead to overloading which would result in impairment of a structure, or on the contrary, in reduction of detrimental effects related to the rapid hydration. Either way, the evolution of concrete microstructure as a limiting factor in the construction process has to be determined in advance which necessitates development of a model for solidifying and further hardening concrete. In order to develop a reasonable material model it is also necessary to be able to obtain at least a small number of material parameters experimentally, which in the case of solidifying concrete presents a challenge. For its relevance to the current situation in the building industry the modeling and experimental work on concrete at the extremely early ages was chosen as the topic of this work.

The material modeling presented here is derived from the solidification theory presented by Prof. Bažant in [1]. Firstly, some considerations on microstructure evolution of concrete are discussed. Secondly, the basic concept of the material model for concrete at very early ages is described. The modification of Chen model of plasticity, [2], originally derived for the already hardened concrete, is then presented as an example of possible approach to extension of the applicability range of material models. Thirdly, suitable testing methods for experimental analysis of solidifying and hardening concrete are presented along with a method developed for measurement of lateral deformation of concrete specimen subjected to uniaxial loading, which is based on processing of digital images. Fourthly, examples of application of the modified Chen model of plasticity and the experimentally obtained data to solution of two real structural problems are presented.

2. MODELING OF CONCRETE AT VERY EARLY AGES

2.1 Evolutionary change in concrete at very early ages

The evolution of microstructure of concrete is a physicochemical process which depends on many factors of varying importance. Eliminating the outdoor factors, such as climatic conditions, by maintaining constant ambient temperature and humidity or establishing fully adiabatic conditions, the effect of the intrinsic factors related to the chemical composition of constituents can be observed. The chemical reaction at the microscopic level depends mainly on chemical composition and amounts of concrete constituents, which are roughly, however sufficiently, described by the water-cement ratio, the type and fineness of cement and mix proportions. In order to introduce the effects related to internal material changes to the material model, it is necessary to choose a suitable internal variable. The degree of hydration is an internal variable whose concept is commonly accepted and which implicitly involves the physicochemical considerations.

As was mentioned, the degree of hydration as the measure of progress in the development of microstructure also needs to reflect effects of outer influencing factors, such as climatic conditions. For this reason the degree of hydration is also a function of temperature and of the amount of free water in pores. Time, as a variable, has to be incorporated since time plays the role of a reference which is used for relating the external effects to the model, such loading and changes in climatic conditions.

The evolutionary change is described by the degree of hydration, which is defined by the following equation

$$h = f(\alpha_i, t) \qquad (i = 1, \ldots, n), \tag{1}$$

where α_i are coefficients related to the influencing factors and t is time elapsed after mixing water with cement. Among the influencing factors, which need to be taken into account are the cement type, amount of cement, water-cement ratio, aggregate-cement ratio, sand-aggregate ratio and ambient temperature and relative humidity.

An explicit form of h can be introduced in the form of an exponential function

$$\begin{aligned} h &= f(t_n) = a_1 \cdot \left(\exp(t_n a_2)^{a_3} - 1\right), \\ a_1 &= (32W/C - 3.78)/10000, \\ a_2 &= 3.31 + 9.08W/C, \\ a_3 &= 1.31 + 0.74W/C, \end{aligned} \tag{2}$$

where t_n is time normalized with respect to the final setting time and a_i are empirical parameters which depend on the influencing factors and which have to be identified from experiments (Values obtained for concrete made of rapid hardening Portland cement concrete with 28-day compressive strength in the range 30 to 60 MPa are given. *W/C* is the water-cement ratio in decimal). The evolutionary function expressed by Eq. (2) can be used for the ages up to the final setting time. Eq. (2) is shown in Figure 1.

Another explicit form of h, which can be used also for the ages beyond the final setting time, is represented by the following monotonically increasing S-shaped hyperbolic function

$$\begin{aligned} h &= f(t_n) = a_5 \cdot \left(\frac{a_3 {t_n}^{a_2}}{a_1 + a_3 {t_n}^{a_2}} \right)^{a_4}, \\ a_1 &= 10, \\ a_2 &= 9.164 - 7.2W/C, \\ a_3 &= 0.72, \\ a_4 &= 1, \\ a_5 &= 15, \end{aligned} \tag{3}$$

where t_n is time normalized with respect to the final setting time and a_i are empirical parameters which depend on the influencing factors and which have to be identified from experiments (Values obtained for concrete made of rapid hardening Portland cement concrete with 28-day compressive strength in the range 30 to 60 MPa are given. *W/C* is the water-cement ratio in decimal). The parameter a_5 is used due to the normalization of the functional value with respect to its value at the final setting time. However, at normal use the parameter a_5 is omitted or its value is 1 because the evolutionary function, same as the degree of hydration, reaches unity at infinity.

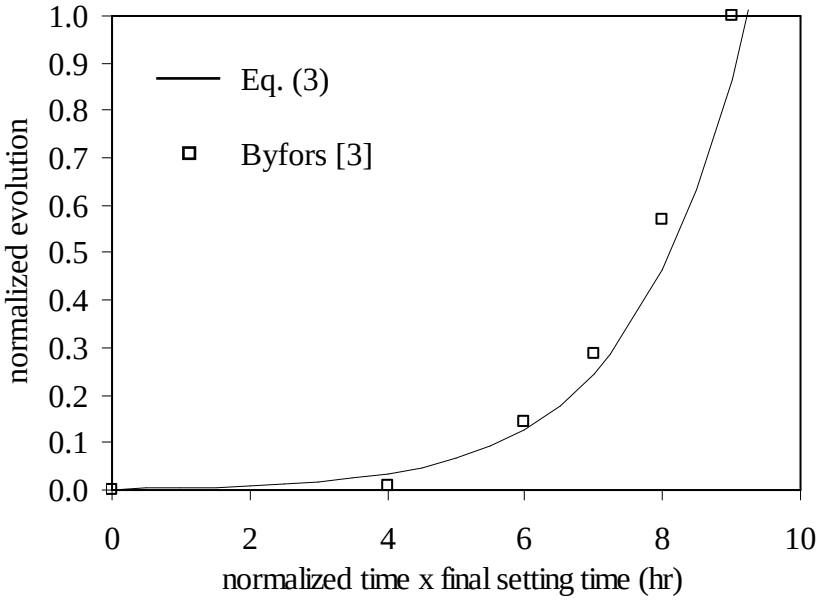

Figure 1: Comparison between normalized evolutionary function and experimental data

2.2 General approach to modeling

In general, the deformational behavior of concrete at very early ages resembles that of already hardened one with the distinction of the pronounced plastic deformability which is at the ages between the initial and final setting times prominent. With the further increasing age the ratio between the irreversible and the reversible deformations decreases, which means, the deformation can be distinguished according to its nature. For that reason, the total strain can be split into four components

$$\varepsilon(t) = \varepsilon^e(t) + \varepsilon^v(t) + \varepsilon^f(t) + \varepsilon^0(t), \tag{4}$$

where ε^e is the elastic or instantaneous strain, ε^v is the reversible viscous strain, ε^f is the irreversible viscous (flow) strain, and ε^0 is the stress-independent strain produced by the hydration process such as autogeneous shrinkage and the thermal strain. The difference between the deformational behavior of hardening concrete and the already hardened concrete is in the pronounced variation in magnitudes of the strain components. At the ages ranging from the time of mixing until about the initial setting time, the irreversible viscous strain component, ε^f, prevails. With progressing hydration the elastic component, ε^e, and the reversible viscous, ε^v, components are more pronounced while prevalence of the irreversible viscous strain component, ε^f, recedes. The strain component related to the hydration process and stress-independent influences, ε^0, is of varying importance throughout the solidification process, which is attributed to the increase of tensile strength of concrete.

The main difference between the hardening concrete and the already hardened one, especially noticeable under sustained loading, is the significant change in the material parameters due to the hydration process which no longer allows the simplifying assumption that material parameters are constant during the whole length of loading. It also should be pointed out that in the case of hardened concrete which is loaded at higher ages the duration of sustained loading can be, and usually is, measured as the time elapsed from the instant of loading until the moment of interest, which is in accordance with the assumption of the

constant material parameters. In the case of hardening concrete, duration of sustained loading is actually prescribed in terms of time, however, for modeling it is more convenient to express the duration of sustained loading in terms of the degree of hydration, proposed above, allowing more general considerations which cannot be expressed as a mere time duration. This is, for instance, the effect of elevated temperature due to hydration which further accelerates hydration process and which results in relative contraction of the loading period. Therefore, for the uniaxial response to uniaxial loading, the strain should be expressed by

$$\varepsilon(t) = \int_0^t J(t,t',h,h')d\sigma(t'), \tag{5}$$

where J is the compliance function, h is the degree of hydration at the moment of interest, t, and h' is the degree of hydration at the instant of loading, t', ε is strain and σ is stress. The compliance function J is a function of the internal variable, the degree of hydration, on the level of definition of the model, however, on the outside the compliance function J is a function of time. This is consistent since there is a one-to-one mapping between the internal variable and time for given conditions. The strain, ε, in Eq. (5) represents the sum of the first three components in Eq. (4), excluding the strain component ε^0.

Eq. (5) can be differentiated with respect to time, t, which results in

$$\frac{d\varepsilon(t)}{dt} = J(t,t)\frac{d\sigma(t)}{dt} + \int_0^t \frac{\partial J(t,t')}{\partial t} d\sigma(t'), \tag{6}$$

where $J(t,t)$ in the first term in Eq. (6) represents the instantaneous modulus of elasticity related to the elastic strain, ε^e, in Eq. (4) as a function of the degree of hydration, h, at time t. The second term in Eq. (6) can be further decomposed into two parts

$$\int_0^t \frac{\partial J(t,t')}{\partial t} d\sigma(t') = \int_0^t \left(\frac{\partial J^v(t,t')}{\partial t} + \frac{\partial J^f(t,t')}{\partial t} \right) d\sigma(t'), \tag{7}$$

where J^v is the creep function related to the reversible viscous strain, ε^v, and J^f is the creep function related to the irreversible viscous flow strain, ε^f.

Eq. (4) can be rewritten as a rate-type relation

$$\dot{\varepsilon}(t) = \dot{\varepsilon}^e(t) + \dot{\varepsilon}^v(t) + \dot{\varepsilon}^f(t) + \dot{\varepsilon}^0(t), \tag{8}$$

where the meaning of all entries is identical with those in Eq. (4) and the superposed dot indicates the differentiation with respect to time. The exact definition of each component is given in the following. The strain component ε^0 is not dealt with in this work.

The elastic strain rate is given by

$$\dot{\varepsilon}^e(t) = \frac{F_0[\sigma(t),\dot{\varepsilon}(t)]\dot{\sigma}(t)}{E(t)}, \tag{9}$$

where $E(t)$ is the instantaneous modulus of elasticity and $F_0[\sigma(t), \dot{\varepsilon}(t)]$ is a function which expresses the effect of large stresses and the effect of loading rate. The instantaneous modulus of elasticity, $E(t)$, can be assumed to be proportional to the microstructural evolution which is expressed by the degree of hydration and defined as

$$E(t) = E_0 h(t), \tag{10}$$

where E_0 is an empirical constant and h is a function representing the evolution of microstructure related to the instantaneous response, such as the degree of hydration.

The elastic deformation comprises the deformation of the solid particles of sand and aggregate, the deformation of water and the deformation of the already hardened cement paste and the not yet hydrated cement grains. These particles can be considered to be nonaging constituents of concrete, which is consistent from the physicochemical point of view once the effect of aging is dealt with separately. The aging can be defined, e.g., as a variation of proportions among the constituents or a ratio between an instant value of a quantity and the value of the quantity when the hydration is completed known as the degree of hydration.

The reversible viscous strain represents the strain component which later for the hardened concrete becomes the strain usually described as the viscoelastic. For the sake of consistency of the description of the deformation for both the hardening and hardened concrete, the reversible viscous strain component is used for description of the deformation of the hardening concrete, especially the time-dependent, which in its nature resembles that of the already hardened concrete. Even though the term reversible is used as the name of this strain component, in the case of the solidifying and hardening concrete the reversible part of the deformation is negligible when compared with the irreversible part. This reasoning is justified by the experimental data obtained by the author [4, 5] and also by the method of the description of creep of concrete at the very early ages (2 to 7 hours) adopted by Okamoto in [6]. In his work Okamoto used the viscoelastic three- and four-element rheological models without any clear explanation about the possible reversibility of the creep deformation. This may have been for the reason that there were no experimental data on cyclic loading available at that time.

The reversible viscous strain rate is expressed as follows

$$\dot{\varepsilon}^{v}(t) = \frac{F_1[\sigma(t), \dot{\varepsilon}(t)]}{\alpha h(t)} \int_0^t \dot{J}^{v}(t,t') d\sigma(t'). \tag{11}$$

In Eq. (11) $J^{v}(t,t') = J^{v}(t-t')$ is the creep function related to the reversible viscous strain component and it is considered to be a function of the elapsed time during the period when load is applied, which means, $J^{v}(t,t')$ is a non-aging material parameter independent of age. The effect of the progressing hydration which controls evolution of the microstructure of the hardening concrete is prominent at the age when concrete solidifies and further hardens and so it needs to be included in the modeling. This effect can be expressed directly by an evolutionary function related to the reversible viscous strain, $h(t)$, multiplied by an empirical constant, α, as seen in the denominator preceding the integral in Eq. (11). The effect of higher stresses is known to cause an increase in strain rate which is evidenced as the nonlinear deformational behavior. This effect can be included in the description of the reversible viscous strain as a non-dimensional parameter which is a function of the instant stress level at the moment of loading. The strain rate does not affect the reversible viscous component significantly, partially because this strain component is used mainly for description of the response under sustained loading, nevertheless, it is also considered in the modeling. Both the effects of a higher stress level and a strain rate are expressed by $F_1[\sigma(t), \dot{\varepsilon}(t)]$ in the numerator preceding the integral in Eq. (11).

Because the viscous deformation of the solidifying and hardening concrete is mainly irreversible, the irreversible viscous strain is the most useful component for both the

responses under short-time and sustained loading. The irreversible viscous strain rate is formulated similarly to the reversible viscous strain and is expressed by

$$\dot{\varepsilon}^{f}(t) = F_2[\sigma(t), \dot{\varepsilon}(t)] \int_0^t \dot{J}^{f}(t,t')d\sigma(t'), \tag{12}$$

where $J^{f}(t,t') = J^{f}(t-t')$ is the creep function related to the irreversible viscous strain component and the function $F_2[\sigma(t), \dot{\varepsilon}(t)]$ expresses the effect of large stresses and the effect of loading rate.

Assuming a linear dependence of the irreversible viscous strain rate on the stress, the integral in Eq. (12) can be transformed into

$$\int_0^t \dot{J}^{f}(t,t')d\sigma(t') = \frac{\sigma(t)}{\eta(t)}, \tag{13}$$

where $\eta(t)$ is the plastic viscosity which can be defined as a function of an evolutionary function with a similar meaning to the degree of hydration. Also in the case of the plastic viscosity, $\eta(t)$, it can be assumed that the evolution of the plastic viscosity is proportional to the evolution of microstructure and the plastic viscosity can be defined as

$$\eta(t) = \beta h(t), \tag{14}$$

where β is an empirical constant and $h(t)$ is an evolutionary function related to the irreversible viscous strain. Then, Eq. (12) can be written as

$$\dot{\varepsilon}^{f}(t) = \frac{F_2[\sigma(t), \dot{\varepsilon}(t)]}{\beta h(t)}\sigma(t). \tag{15}$$

In order to improve the predictive capability of the model it is desirable to introduce the effect of loading rate into the model. It is known that a higher loading rate causes relative stiffening of concrete which is caused by suppression of time-dependent deformation. Also, the nonlinearity which occurs at higher stress levels should not be neglected especially for the stress levels exceeding 50 per cent. Particularly in the case of hardening concrete, higher stress levels are common due to the yet developing microstructure. The rapid development of microstructure during solidification and hardening also causes a significant decrease of the load level when the solidifying or hardening concrete is subjected constant loading which once left unaccounted for would lead to overestimation of the time-dependent deformation. The effect of high stress levels and loading rate can be jointly expressed by

$$F_i[\sigma(t), \dot{\varepsilon}(t)] = F_{Li}F_{Ri}, \tag{16}$$

where $F_i[\sigma(t), \dot{\varepsilon}(t)]$ is defined as a product of a function F_{Li} representing the effect of a higher load level and a function F_{Ri} representing the effect of loading rate. The index, i, implies that the functions F_{Li} and F_{Ri} may not be the same for all strain components. The function $F_i[\sigma(t), \dot{\varepsilon}(t)]$ can be identified from experimental data.

The governing equation of the proposed model which describes the deformational behavior of hardening concrete subjected to uniaxial loading can be written as the sum of the

strain components, which were defined above. The strain component ε_0 is also included in the governing equation. In the case of constant stress, which is applied at time *t'*, the governing equation of the proposed model can be expressed in an incremental form by Eq. (17) and in absolute values by Eq. (18).

$$\dot{\varepsilon}(t,t') = \left\{ F_1[\sigma(t),\dot{\varepsilon}(t)] + \frac{\dot{J}^v(t,t')}{\alpha h(t)} + \frac{F_2[\sigma(t),\dot{\varepsilon}(t)]}{\beta h(t)} \right\} \sigma(t) + \dot{\varepsilon}^0(t) \tag{17}$$

$$\begin{aligned} \varepsilon(t,t') \;=\; & \left\{ \frac{F_0[\sigma(t),\dot{\varepsilon}(t)]}{E_0 h(t)} + \int_0^t \left(F_1[\sigma(t),\dot{\varepsilon}(t)] \frac{\dot{J}^v(t,t')}{\alpha h(t)} + \right. \right. \\ & \left. \left. + \frac{F_2[\sigma(t),\dot{\varepsilon}(t)]}{\beta h(t)} \right) dt \right\} \sigma(t) + \varepsilon^0(t) \end{aligned} \tag{18}$$

whose parameters are described above.

The proposed uniaxial model for the deformational behavior of solidifying and hardening concrete is extended to its three-dimensional form so that the model can be also applied to multi-dimensional analyses.

For a general three-dimensional analysis Eq. (4) becomes

$$\dot{\boldsymbol{\varepsilon}}(t) = \dot{\boldsymbol{\varepsilon}}^e(t) + \dot{\boldsymbol{\varepsilon}}^v(t) + \dot{\boldsymbol{\varepsilon}}^f(t) + \dot{\boldsymbol{\varepsilon}}^0(t), \tag{19}$$

where $\boldsymbol{\varepsilon}^e$ is the vector of elastic or instantaneous strains, $\boldsymbol{\varepsilon}^v$ is the vector of reversible viscous strains, $\boldsymbol{\varepsilon}^f$ is the vector of irreversible viscous (flow) strains, and $\boldsymbol{\varepsilon}^0$ is the vector of strains produced by the hydration process such as thermal strain, autogeneous shrinkage and cracking strain.

The creep Poisson's ratio, necessary for multi-dimensional analyses, is in general a function of time, or of the degree of hydration. For hardened concrete, the creep Poisson's ratio is assumed constant and is replaced by the Poisson's ratio, based on the experimental data. This assumption simplifies the three-dimensional creep analysis, and it is only necessary to use the uniaxial response function.

2.3 Modification of Chen model of plasticity

Chen model of plasticity is a three-parameter model for concrete displaying isotropic hardening [2]. This model expresses the elastoplastic behavior of concrete. The typical behavior of concrete is represented by the varying stress-strain characteristics under tension and compression. Two different, but similar, functions were proposed for each of the loading surfaces, in the compression-compression region and in the tension-tension or tension-compression region.

The loading function f_c valid in the compression area is a parabola. The loading function f_t defined in the tension-tension and tension-compression area is a hyperbola. Since these parts of the loading function are different, it is important to determine the correct stress-state zone. The zoning of the biaxial stress states is shown in the (σ_1, σ_2) space in Figure 2.

The curves in Figure 2 represent two extreme situations. The inner curve represents the initial yield surface defined by the initial yield stresses f_{yc} in compression, f_{yt} in tension and f_{ybc} in biaxial compression. The outer curve represents failure surface defined with ultimate

stresses; f_c in compression, f_t in tension and f_{bc} in biaxial compression. An expansion of initial yield surface leads to subsequent loading surfaces.

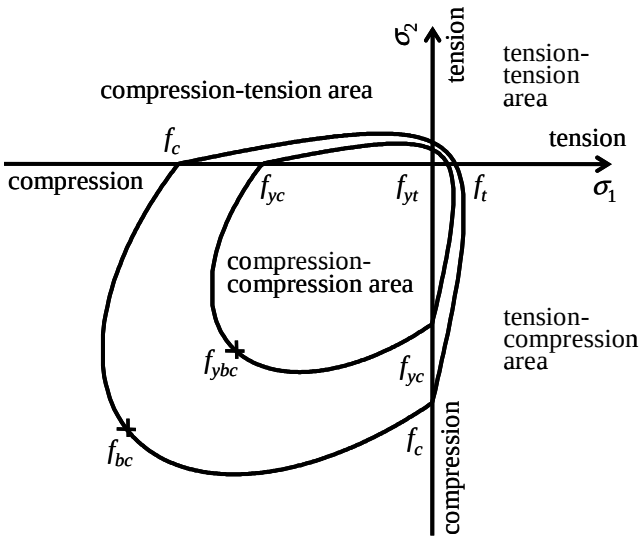

Figure 2: Biaxial stress space

Figure 3 shows the loading surfaces for general stress states in the (σ_1, σ_2, σ_3) space. Also here the two extreme situations, initial yield surface and failure surface, again can be seen. For the triaxial loading of concrete it is not easy to select the correct stress-state zone, as in the case of the biaxial loading. The appropriate region for the general stress-state is determined according to the first invariant of stress tensor I_1 and the second invariant of stress deviator tensor J_2.

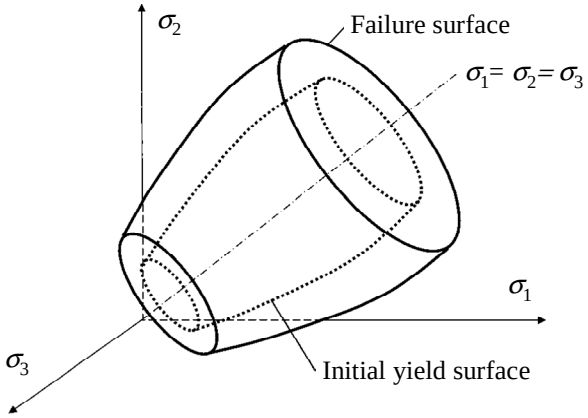

Figure 3: Triaxial stress space

In our example, compression loading is considered hence only the equations for the compression-compression region are introduced in the text.

The failure surface is assumed in the compression-compression region

$$f_u^c(\sigma, h) = J_2 + \frac{A_u(h)}{3} I_1 - \tau_u^2(h) = 0\,. \tag{20}$$

The initial yield surface in the compression-compression region is given by

$$f_0^c(\sigma,h) = J_2 + \frac{A_0(h)}{3} I_1 - \tau_0^2(h) = 0, \tag{21}$$

where $A_0(h)$, $\tau_0(h)$, $A_u(h)$ and $\tau_u(h)$ are material constants which can be determined from simple tests. They are determined as functions of the ultimate stresses under uniaxial compression, $f_c(h)$, and under equal biaxial compression, $f_{bc}(h)$, and of the initial yield stresses under similar conditions, $f_{yc}(h)$ and $f_{ybc}(h)$. The following relations are then used.

$$\begin{aligned} A_0(h) &= \frac{f_{ybc}^2(h) - f_{yc}^2(h)}{2 f_{ybc}(h) - f_{yc}(h)} \\ \tau_0^2(h) &= \frac{f_{yc}(h) f_{ybc}(h)(2 f_{yc}(h) - f_{ybc}(h)}{3(2 f_{ybc}(h) - f_{yc}(h))} \end{aligned} \tag{22}$$

$$\begin{aligned} A_u(h) &= \frac{f_{bc}^2(h) - f_c^2(h)}{2 f_{bc}(h) - f_c(h)} \\ \tau_u^2(h) &= \frac{f_c(h) f_{bc}(h)(2 f_c(h) - f_{bc}(h)}{3(2 f_{bc}(h) - f_c(h))} \end{aligned} \tag{23}$$

All material parameters used in the previous equations are dependent on the function of the microstructure evolution, *h*. Therefore, it is obvious that the loading surfaces are changing with increasing time. With increasing strength of concrete the loading surfaces are expanding.

This is evidenced in Figure 4, where the dotted lines denote the initial yield surface and the failure surface at the age of 7 hours and the solid lines denote the initial yield surface and the failure surface at the age of 9 hours.

The modified Chen model of plasticity was implemented to the existing open program SIFEL, see [7].

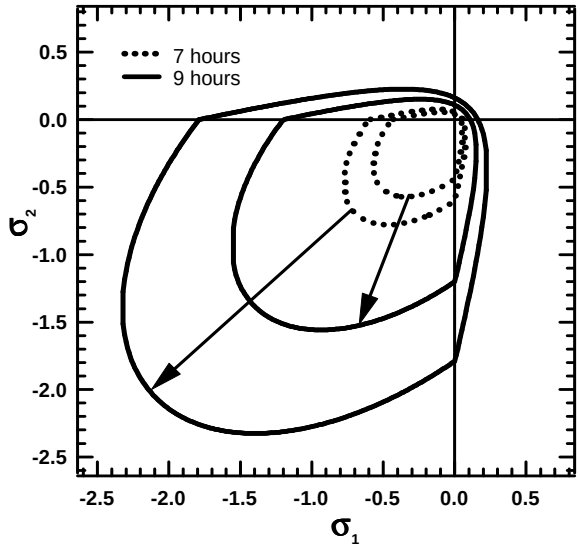

Figure 4: Evolution of initial yield and failure surface strengths

3. RECOMMENDED EXPERIMENTAL METHODS

3.1 Methods based on uniaxial loading

The process of selection of a suitable testing method involves considerations about the possible outcome of an experiment and to what extent the results can be applied to the modeling. The following methods are applicable at the very early ages. The pullout test in which a steel plate is pulled out of solidifying and hardening concrete, the penetration test when a steel needle is driven into the solidifying and hardening concrete, and the uniaxial compression test known from testing the already hardened concrete. The equipment which was used in the three testing methods is schematically described in Figure 5.

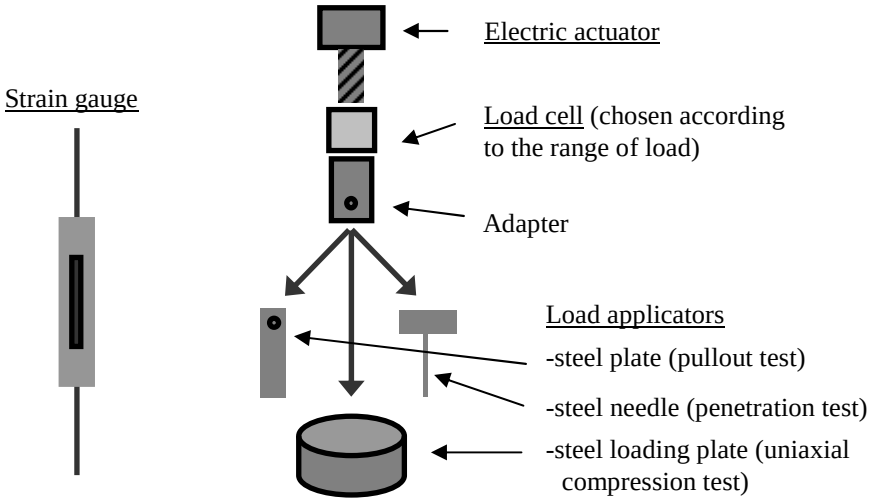

Figure 5: Schematic description of testing equipment

The first two testing methods can be used at anytime during the solidification process. The uniaxial compression test contains the limitation related to the necessity of demolding the specimen before testing. Nevertheless, a methodology was developed which minimized this effect, shown in Figure 6.

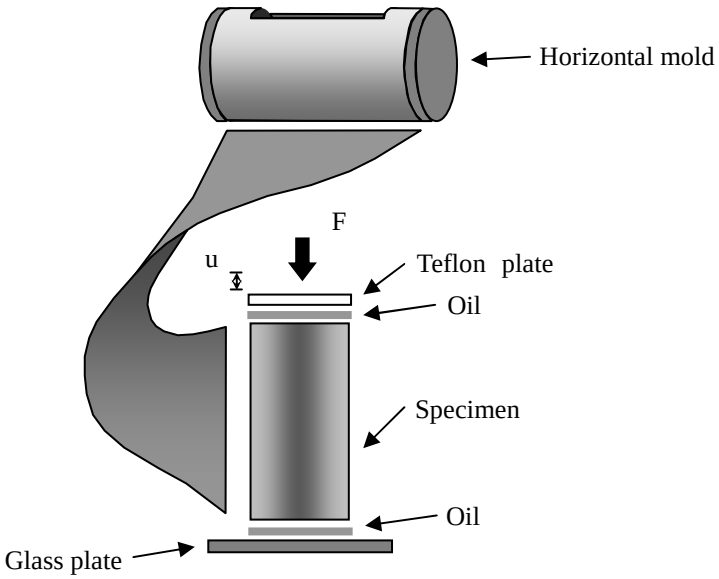

Figure 6: Handling of specimen at extremely early ages

3.2 Image-processing-based method for measuring lateral deformation

Due to the soft consistency of hardening concrete (age of about 4 to 8 hours counted from the instant when water touches cement), use of the contact methods, which are common in experiments with already hardened concrete, is impossible. The method of our choice is based on processing of digital images captured during loading by a high-resolution CMOS camera. The setup of the originally developed method is shown in Figure 7. In this method, the image of the specimen alone is captured.

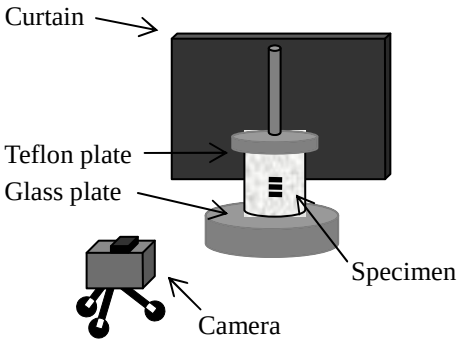

Figure 7: Setup of original method

The developed image processing method is based on searching for the greatest differences in gray shades of the neighboring pixels. The gray scale difference was further refined with the center of gravity method, which delivered a result on the subpixel domain. In order to pronounce the edges of the specimen, a dark curtain was installed behind the original test set and the specimen was illuminated by two spotlights from each side. The focus of the camera was then kept fixed throughout the experiment. The flow chart of the image processing method developed and used with the original test setup is shown in Figure 8. The method was programmed in C and Matlab. More about this method can be found in [8] and more generally on the image processing tools in, e.g. [9].

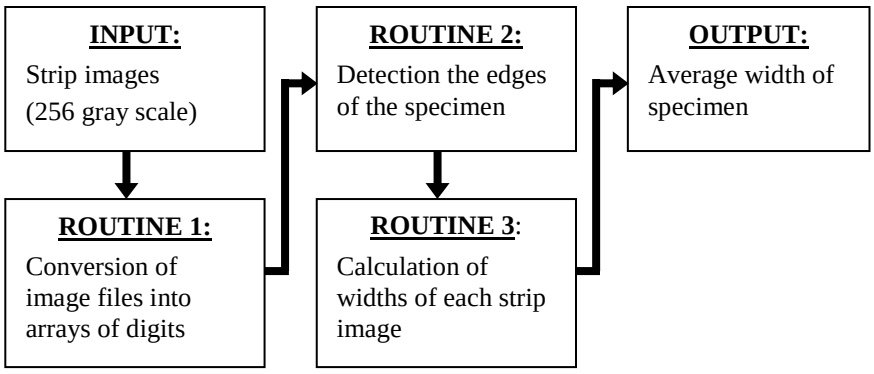

Figure 8: Flow chart of image processing

The experiments took place at the age of about 4 to 8 hours, when hardening concrete still contains a large amount of free water. During loading the free water was squeezed out of the specimen to its surface which resulted in a glistening effect caused by the spotlights. The glistening effect made the specimen appear slimmer than it actually was. This presented an inherent drawback, which, however, affected only the data for the load level below 20 %, as can

be seen in Figure 10. It was attempted to overcome this drawback by introduction of various corrective measures, but none was fit for general use in combination with the original test setup.

Therefore, the setup was modified so that the shadow of the specimen was captured instead of the specimen. The modified setup is schematically depicted in Figure 9. The modified method not only overcame the drawback related to the glistening of the squeezed-out water on the illuminated surface of the specimen, it also allowed incorporation of the thin layer of the squeezed-out water into the measured lateral deformation. Concrete is a composite which comprises cement, sand, aggregate and water. Therefore, the squeezed-out water represents a legitimate component of the lateral deformation.

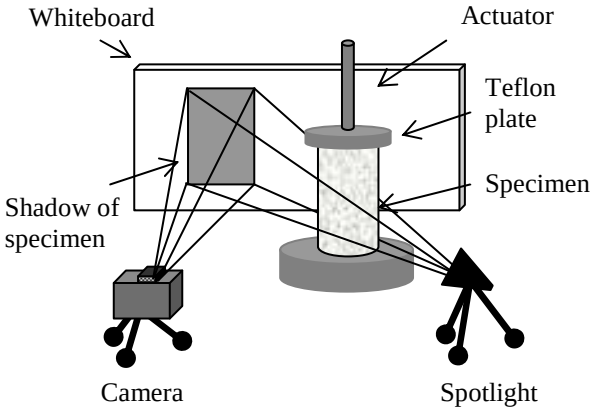

Figure 9: Modified test setup

The obtained results are shown in Figure 10 as a relation between the apparent Poisson's ratio and the load level (defined as the ratio between the applied stress, f, and the compressive strength at the instant of loading, f_c).

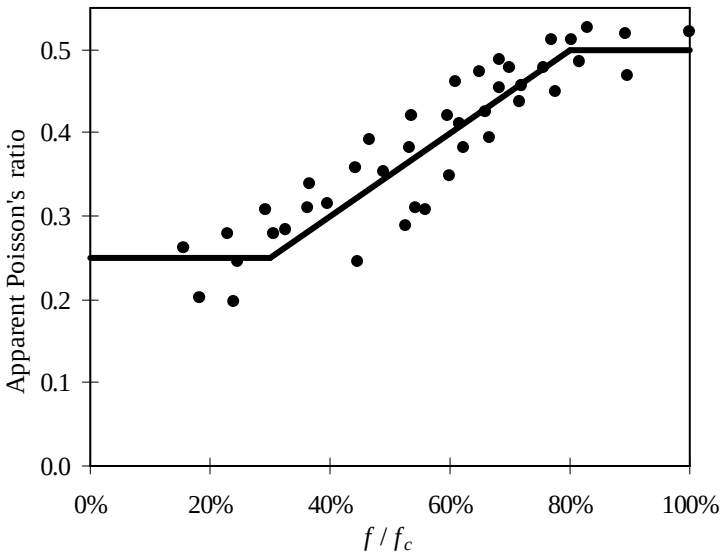

Figure 10: Apparent Poisson's ratio vs. load level of hardening concrete

The solid tri-linear curve indicated in Figure 10 represents a formula which can be readily used in multi-dimensional analyses of hardening concrete. In the formula (24), μ is the apparent Poisson's ratio and $S = f / f_c$.

$$\begin{aligned} \mu(S) &= 0.25 && S \in \langle 0;0.3) \\ \mu(S) &= 0.25 + 0.5(S - 0.3) && for \quad S \in \langle 0.3;0.8) \\ \mu(S) &= 0.5 && S \in \langle 0.8;1) \end{aligned} \tag{24}$$

4. EXAMPLES OF APPLICATION

4.1 Deformation of bridge deck during construction

The Border bridge is a part of the newly constructed D8 highway connecting Prague (Czech Republic) and Dresden (Germany). This composite bridge is about 500 meters long and overpasses a deep valley, see Figure 11. The intermediate columns are circa 50 meters tall, which prohibits pumping concrete directly from the bottom of the valley to the bridge

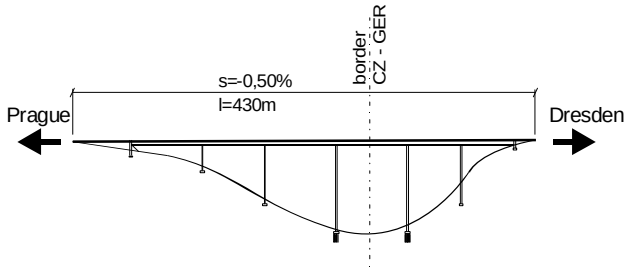

Figure 11: The Border bridge

deck, which is designed as a reinforced concrete slab. Therefore, the concrete needs to be transported to the location of placement across the already finished reinforced concrete deck. As falling behind schedule was very possible threat, especially when the construction site was located in a mountainous area, where it was a subject to unfavorable weather conditions, a tool for estimation of the earliest possible entrance to the newly concreted section of the deck was desirable, moreover, when the tool also provided some information on the possible damage caused by premature loading.

Table 1: Strength characteristics of hardening concrete in MPa

Age of concrete	f_{yc}	f_c
6 hours	0.46094	0.76823
7 hours	0.66242	1.10404
8 hours	0.89387	1.48979
9 hours	1.15042	1.91736
10 hours	1.42726	2.37877
11 hours	1.71994	2.86657
12 hours	2.02442	3.37404
14 hours	2.65513	4.42522
18 hours	3.93361	6.55601
24 hours	5.72713	9.54522

The material characteristics of concrete in the early ages are obtained from experiments with simple techniques based on the uniaxial compression and penetration tests, [10, 11], see Table 1. Also, the experimental data gathered by Byfors yielded, from today's point of view,

very useful data on the evolution of modulus of elasticity and compressive strength of solidifying and further hardening concrete, [3].

Table 1 summarizes the yield stresses and the ultimate stresses from experimental data for concrete of the ages of 6 to 24 hours. Chen in his paper [12] introduced formulas acquiring material parameters for his model from the uniaxial compressive strength. Even if only the ultimate stress in compression is known, it is possible to calculate the remaining values from the following simple formulas

$$\begin{aligned} f_t &= 0.09\, f_c, \\ f_{bc} &= 1.16\, f_c, \\ f_{yc} &= 0.6\, f_c, \\ f_{yt} &= 0.054\, f_c = 0.09\, f_{yc}, \\ f_{ybc} &= 0.6\, f_{bc} = 1.16\, f_{yc}. \end{aligned} \tag{25}$$

From Table 1 it is obvious that the yield stress is approximately equal to 60 %, which is in accord with the corresponding equations (25). Therefore, the application of the relations (25) is justified for our use. In the example presented, the compression-compression area only is dealt with and so it is sufficient to calculate the biaxial yield and ultimate strength in addition to the experimentally obtained uniaxial compressive strength.

This experimental data were used for investigation of the reinforced concrete deck of the composite bridge, where a section of the concrete deck (see Figures 12 and 13) under compression was modeled and analyzed at the ages from 6 to 24 hours. Figures 12 and 13 show deformation of the hardening concrete under the excessive compressive load.

The main objective was to describe the behavior of the concrete deck under compressive load corresponding to the truck carrying fresh concrete. The data for loading force were obtained at a construction site and compared with Eurocode [13]. The force representing the truck tire is 90 kN for one wheel axis.

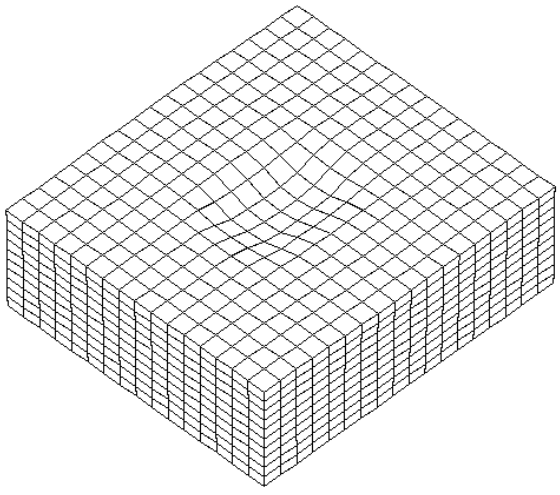

Figure 12: Section of analyzed concrete deck under the front wheel - deformation

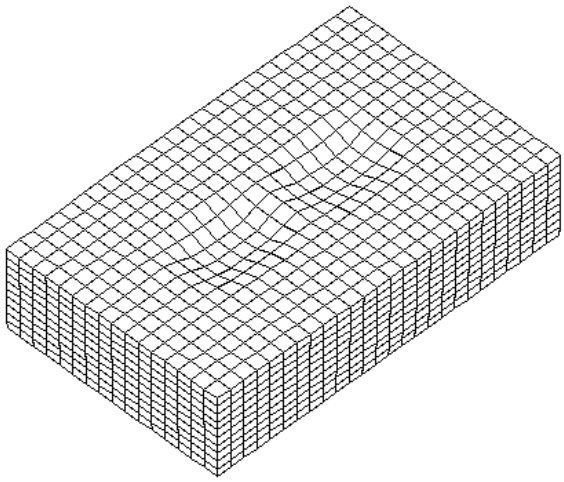

Figure 13: Section of analyzed concrete deck under the rear wheel – deformation

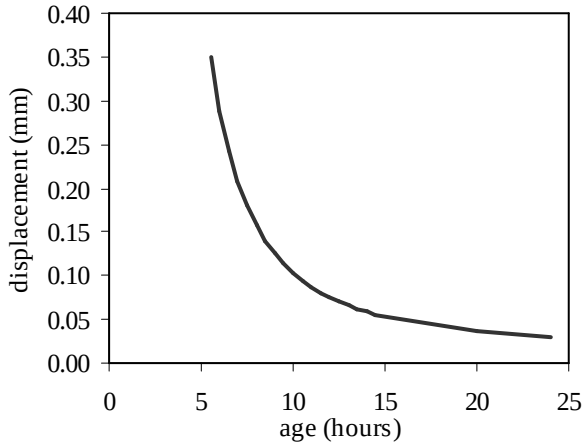

Figure 14: Vertical displacement at various ages

For the front axis, the pressure on the slab was derived from a force of 45 kN. The standard value of the contact area under the wheel was circa 20 x 30 cm. In the case of the rear axis, the pressure on the slab was derived from a force of 22.5 kN for each of the four contact areas. The dimension of the contact area was also 20 x 30 cm.

Figure 14 shows results of the analysis, where the decreasing displacement with increasing age of the concrete under constant loading can be seen. The effect of increasing strength at the ages from 6 to 12 hours is prominent in this graph.

4.2 Rate of pouring concrete in tall RC wall

During construction of Letňany subway station in Prague, a situation occurred when it was necessary to decide the maximum possible rate of pouring concrete in a reinforced concrete wall, which was 10.75 meters tall. The reasoning was not related to the stiffness of the formwork, but to the new expansion joint filler and the vague description of its material properties provided by distributor. The expansion joint filler was 40 mm thick and placed with spacing of 50 m in the wall. The joint filler can be seen as the gray layer on the face of the wall in Figure 15.

Figure 15: Investigated wall with formwork

At this station, use of the classical joint filler made of polystyrene was rejected because of possible chemical degradation of the connecting underground waterproofing membrane. Since the stress-strain diagram of the material provided by distributor was obviously incorrect, additional tests were conducted at Faculty of Civil Engineering of the Czech Technical University in Prague, which confirmed the discrepancy and showed that the stiffness of the material at the decisive region of the stress-strain curve was half of that declared by the distributor. Other important information for the analysis was the mix proportions of concrete and the rate of supply of concrete to the site. The designer expected that concrete could be supplied to the site at 15 m^3 per hour, which meant about 1.25 m per hour increase in height of the placed concrete in the wall. Since the design office allowed only few days for an analysis with quantified results, which put any rigorous multi-dimensional numerical analysis out of question at that time, the following simplified method was adopted.

From Paulini's paper on development of Poisson's ratio over time, [14], it was established that for ages of 4 to 6 hours the value of the Poisson's ratio was about 0.35, which corresponded to the data obtained in our experiments for the load level of about 50 % (Figure 10) and thus it justified the use of the relations in Eq. (24). From Figure 10 and Eq. (24) it was evident that unconfined concrete subjected to load levels above 80 % split and thus it could not support itself. It was assumed that the joint filler provided little confinement compared to the relatively much stiffer formwork and that similar behavior as in Figure 10 obtained from the experiments with unconfined concrete specimens could be expected in the direction normal to the joint filler. Based on the mix proportions of concrete and Eq. (3) the compressive strength evolution of concrete was estimated. Then, for the estimated pouring rate the evolution of vertical load induced by self weight of concrete was calculated. The horizontal stress was estimated from the vertical stress and equation (24), which showed how much concrete could support itself and when it started bulging. The maximum value of the Poisson's ratio was reduced to 0.425, reported by Paulini in [14], which reduced the hydrostatic pressure due to squeezing free water from capillaries to air-filled pores within the microstructure of concrete, which might be less energetically demanding than compressing the joint filler. The calculated horizontal stresses were then used for estimation of deformation of the joint filler using the provided stress-strain diagrams. The results are shown in Table 2, where the original deformation was obtained using the stress-strain diagram provided by the distributor and the updated deformation was obtained with the stress-strain diagram measured at our laboratory.

Table 2: Deformation of expansion joint filler

hour	strength (MPa)	vertical load (MPa)	load/strength	lateral load MPa	orig. def. %	upd. def. %
1	0.00	0.02	15.6	0.01	1	1
2	0.01	0.05	5.9	0.04	4	7
3	0.02	0.08	5.2	0.07	5	19
4	0.05	0.11	2.2	0.09	9	32
5	0.12	0.14	1.2	0.12	22	41
6	0.32	0.17	0.5	0.15	45	46
7	0.60	0.2	0.3	0.06	45	46
8	1.00	0.23	0.2	0.07	45	46
9	1.50	0.27	0.2	0.08	45	46
10	2.20	0.3	0.1	0.09	45	46

5. CONCLUSIONS

Basic concept of modeling of concrete at the extremely early ages can consist in separation of the aging effect or definition of the material parameters as a function of age. A model based on the solidification theory was presented along with two functions describing the evolution in microstructure whose parameters could be obtained from simple experimental measurements. An extension of a model for hardened concrete for use in the very early ages was presented in an example when the material parameters used in the Chen model of plasticity were defined as a function of microstructure evolution. Simple testing methods based on uniaxial testing, which made use of the equipment present in most laboratories, were described and a contact-free method for measuring lateral deformation of a concrete specimen was proposed. Applicability of the modified Chen model of plasticity and the experimentally obtained data was shown in two examples.

Literature

[1] Z.P. Bažant, S. Prasannan. Solidification theory for concrete creep. Journal of Engineering Mechanics, ASCE, 115(8): 1691-1725, 1989.

[2] W.F. Chen. Plasticity in reinforced concrete. Osbourne-McGraw-Hill, New York, 1982.

[3] S.G. Bergström, J. Byfors. Properties of concrete at early ages. 32nd Meeting of RILEM Permanent Committee: 265-274, 1979.

[4] P. Štemberk, T. Tsubaki. Uniaxial deformational behavior and its modeling of solidifying concrete under short-time and sustained loading., Journal of Applied Mechanics, JSCE, 6: 437-444, 2003.

[5] P. Štemberk, T. Tsubaki. Modeling of creep of solidifying concrete at various load levels. Cement Science and Concrete Technology, 57: 223-230, 2003.

[6] H. Okamoto. A study on creep properties of concrete at very early age. 30th Japan Congress on Materials Research: 171-174, 1987.

[7] http://cml.fsv.cvut.cz/~sifel/index.html

[8] P. Štemberk, A. Kohoutková. Image-analysis-based measuring of lateral deformation of hardening concrete. Materials Science, 11(3): 292-296, 2005.

[9] R. Gonzalez, R. Woods. Digital image processing. Prentice-Hall, Inc., New Jersey, 2002.

[10] I. Monzón Hualde, P. Štemberk, O. Lojkásek. Description of material properties of hardening concrete inside deck of composite bridge. Proc. of Engineering Mechanics 2006, CD-rom: 1-9, 2006.

[11] M. Frantová. Modification of Chen model of plasticity for early ages applications. Mechanika, 58(2): 11-16, 2006.

[12] A.C.T Chen, W.F. Chen. Constitutive equations and punch-indentation of concrete. Journal of the engineering mechanics division, 101(EM6): 889-906, 1975.

[13] EN 1991-1-1: Actions on structures - General actions - Densities, self-weight and imposed loads. European CEN, 04/2002.

[14] P. Paulini, N. Gratl. Stiffness formation of early age concrete. Thermal cracking in concrete at early ages, Eds. R. Springerschmid, E & FN Spon, London, 1994.

Ing. Petr Štemberk, Ph.D.

Katedra betonových a zděných konstrukcí, Fakulta stavební, ČVUT v Praze
Thákurova 7, 166 29 Praha 6, tel: +420-224-354-364, stemberk@fsv.cvut.cz

Education:

1993-1998 M.Sc. study (Civil Engineering)
Czech Technical University in Prague, Faculty of Civil Engineering, Prague, Czech Republic.
Defense of M.Sc. thesis: 6/1998
M.Sc. thesis: Heat and Moisture Transfer in Concrete

1998-2000 Ph.D. study (Civil Engineering)
Czech Technical University in Prague, Faculty of Civil Engineering, Prague, Czech Republic.
Defense of Ph.D. thesis: 9/2000
Ph.D. thesis: Fuzzy Set Theory - Applications

2000-2003 Ph.D. study (Civil Engineering, Architecture and Marine Technology)
Yokohama National University, Yokohama, Japan.
Defense of Ph.D. thesis: 9/2003
Ph.D. thesis: Evolutionary Material Model of Hardening Concrete under Uniaxial Loading

Professonal position:

2003-present Assistant Professor in Department of Concrete and Masonry Structures, Czech Technical University in Prague, Faculty of Civil Engineering

Teaching activity:

Design of concrete structures
Design of masonry structures
Concrete technology

Research activity:

Special interest in thermodynamics of concrete, methodology of testing of solidifying and hardening concrete, material modeling of concrete and incorporation of uncertainties in material description based on soft computing and fuzzy set theory.
Project leader of research projects: GAČR 103/04/1320 (Application of fuzzy set theory in modeling of material uncertainties in concrete structures, 2005-2006), GAČR 103/05/2244 (Experimental methods for investigation of concrete loaded at extremely early ages and its modeling, 2005-2007) and GAČR 103/07/1462 (Fuzzy-logic-based system for evaluation of construction procedures for concrete structures, 2007-2009).
Representative of Association for Advancement of Modelling and Simulation Techniques in Enterprises for the Czech Republic.